Complexes with Platinum−Iridium Bonds: Stepwise Formation of a $PtIr_2$ Cluster Complex

Brian T. Sterenberg, Hilary A. Jenkins, and Richard J. Puddephatt*

Department of Chemistry, University of Western Ontario, London, Ontario, Canada N6A 5B7

Received August 3, 1998

The reaction of $[Pt(dppm)_2]Cl_2$ (dppm = $Ph_2PCH_2PPh_2$) with $[Ir(CO)_4]^-$ and dppm in a 1:2:1 ratio leads in a multistep reaction to the new heteronuclear cluster complex $[PtIr_2(CO)_2(\mu\text{-}CO)(\mu\text{-}dppm)_3]$, which contains a triangle of metal atoms with each edge bridged by a dppm ligand and in which only the platinum atom is coordinatively unsaturated. The initial step in the reaction leads to formation of the neutral and cationic binuclear complexes $[PtIrCl(CO)_2(\mu\text{-}dppm)_2]$ and $[PtIr(CO)_3(\mu\text{-}dppm)_2]^+$, respectively. The binuclear complexes then react with additional $[Ir(CO)_4]^-$ to form the cluster $[PtIr_2(CO)_4(\mu\text{-}CO)(\mu\text{-}dppm)_2]$ by insertion into a Pt−P linkage; this cluster can exist in two isomeric forms, each containing a triangular $PtIr_2$ group with the Ir−Ir and one Pt−Ir edge bridged by dppm ligands but differing in stereochemistry. These isomers equilibrate slowly at room temperature, and each reacts easily with dppm to form the final cluster complex $[PtIr_2(CO)_2(\mu\text{-}CO)(\mu\text{-}dppm)_3]$. The structures of the complexes $[PtIr_2(CO)_2(\mu\text{-}CO)(\mu\text{-}dppm)_3]$, $[PtIr(CO)_3(\mu\text{-}dppm)_2][PF_6]$, and one isomer of $[PtIr_2(CO)_4(\mu\text{-}CO)(\mu\text{-}dppm)_2]$ have been determined crystallographically, and the reaction sequence has been determined by monitoring reactions through NMR methods.

Introduction

There is interest in heteronuclear cluster complexes containing platinum and iridium,[1] since they have the potential to act as models for bimetallic Pt−Ir-alumina catalysts, one of a group of bimetallic Pt−M catalysts including Pt−Ir, Pt−Re, and Pt−Sn on alumina which are used in petroleum refining.[2] These bimetallic platinum−iridium catalysts have advantages over simple platinum catalysts on alumina in having both improved selectivity for dehydrocyclization rather than cracking of linear alkanes and longer active lifetimes.[3]

Platinum−iridium cluster complexes are relatively uncommon, and improved routes to stable platinum−iridium clusters are clearly needed in order for the reactivities to be studied.[1,4] Recently we described the formation of the cationic Pt_2Ir cluster complex $[Pt_2Ir(CO)_2(\mu\text{-}dppm)_3]^+$ (**2**) by reaction of the dicationic cluster complex $[Pt_3(\mu_3\text{-}CO)(\mu\text{-}dppm)_3]^{2+}$ (**1**) with $[Ir(CO)_4]^-$, as shown in Scheme 1.[1b] This reaction involves the formal substitution of Pt by $\{Ir(CO)\}^-$, so that the 42-electron cluster **1** is converted to the 44-electron cluster **2**, thus allowing platinum and iridium centers to have 16- and 18-electron configurations, respectively. Although a similar displacement of a second platinum atom to form the neutral $PtIr_2$ cluster $[PtIr_2(CO)_3(\mu\text{-}dppm)_3]$ (**3**) might be anticipated, the Pt_2Ir cluster failed to react with further $[Ir(CO)_4]^-$ (Scheme 1). This paper reports a route to $PtIr_2$ clusters, including **3**, by the reaction of the mononuclear complex $[Pt(dppm)_2]^{2+}$ with $[Ir(CO)_4]^-$. The use of metal carbonylate anions in the construction of clusters is well-established,[5] and the present example is of interest because it occurs in a stepwise mechanism; the heterobinuclear platinum−iridium intermediates have also been characterized. A particularly clear picture of the cluster growth mechanism is therefore obtained.

Results and Discussion

The overall reaction sequence for formation of **3** is shown in Scheme 2, and the reactions involved are discussed below.

Formation of the $PtIr_2$ Cluster Complex $[PtIr_2(CO)_2(\mu\text{-}CO)(\mu\text{-}dppm)_3]$ (3). The reaction of $[Pt(dppm)_2]Cl_2$ with $[PPN][Ir(CO)_4]$ and dppm in a 1:2:1 ratio led to the formation of the dark red cluster $[PtIr_2(CO)_2(\mu\text{-}CO)(\mu\text{-}dppm)_3]$ (**3**), which has been characterized by spectroscopy and by an X-ray structure determination.

The ^{31}P NMR spectrum of **3** contains three complex ^{31}P resonances at δ −16.3, −28.6, and −45.7, assigned to phosphorus atoms P^a, P^b, and P^c, respectively, as

(1) (a) Spivak, G. J.; Yap, G. P. A.; Puddephatt, R. J. *Polyhedron* **1997**, *16*, 3861. (b) Sterenberg, B. T.; Spivak, G. J.; Yap, G. P. A.; Puddephatt, R. J. *Organometallics* **1998**, *17*, 2433.

(2) (a) Guczi, L. In *Metal Clusters in Catalysis*; Gates, B. C., Guczi, L., Knozinger, H., Eds.; Elsevier: New York, 1986. (b) Farrugia, L. J. *Adv. Organomet. Chem.* **1990**, *31*, 301. (c) Adams, R. D.; Hermann, W. A. *Polyhedron* **1988**, *7*, 2255. (d) Sinfelt, J. H. *Bimetallic Catalysts: Discoveries, Concepts and Applications*; Wiley: New York, 1983. (e) Xiao, J.; Puddephatt, R. J. *Coord. Chem. Rev.* **1995**, *143*, 457.

(3) (a) Rasser, J. C.; Beindorff, W. H.; Scholten, J. J. F. *J. Catal.* **1979**, *59*, 211. (b) Rice, R. W.; Lu, K. *J. Catal.* **1982**, *77*, 104. (c) Yang, O. B.; Woo, S. I.; Ryoo, R. *J. Catal.* **1992**, *137*, 357.

(4) (a) Bhaduri, S.; Sharma, K. R.; Clegg, W.; Sheldrick, G. M.; Stalke, D. *J. Chem. Soc., Dalton Trans.* **1984**, 2851. (b) Freeman, M. J.; Miles, A. D.; Murray, M.; Orpen, A. G.; Stone, F. G. A. *Polyhedron* **1984**, *3*, 1093. (c) Fumagalli, A.; Pergola, R. D.; Bonacina, G.; Garlaschelli, L.; Moret, M.; Sironi, A. *J. Am. Chem. Soc.* **1989**, *111*, 165. (d) Stang, P. J.; Huang, Y. H.; Arif, A. M. *Organometallics* **1992**, *11*, 845. (e) Balch, A. L.; Catalano, V. J. *Inorg. Chem.* **1992**, *31*, 2569. (f) Hadj-Bagheri, N.; Puddephatt, R. J. *Inorg. Chim. Acta* **1993**, *213*, 29. (g) Tanase, T.; Toda, H.; Kobayashi, K.; Yamamoto, Y. *Organometallics* **1996**, *15*, 5272.

(5) (a) Garlaschelli, L.; Della Pergola, R.; Martinengo, S. *Inorg. Synth.* **1989**, *28*, 211. (b) Mingos, D. M. P.; Wales, D. J. *Introduction to Cluster Chemistry*; Prentice-Hall: Englewood Cliffs, NJ, 1990.

10.1021/om980665y CCC: $18.00
Publication on Web 12/24/1998

Scheme 1

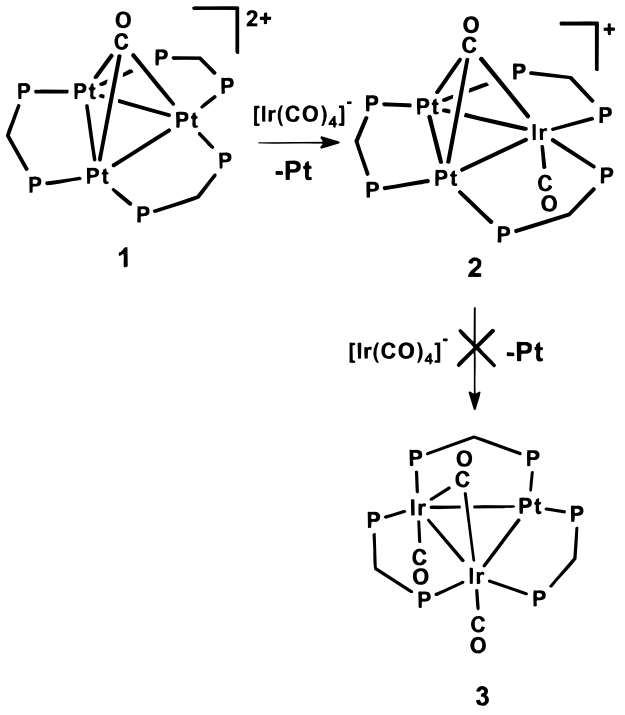

Scheme 2

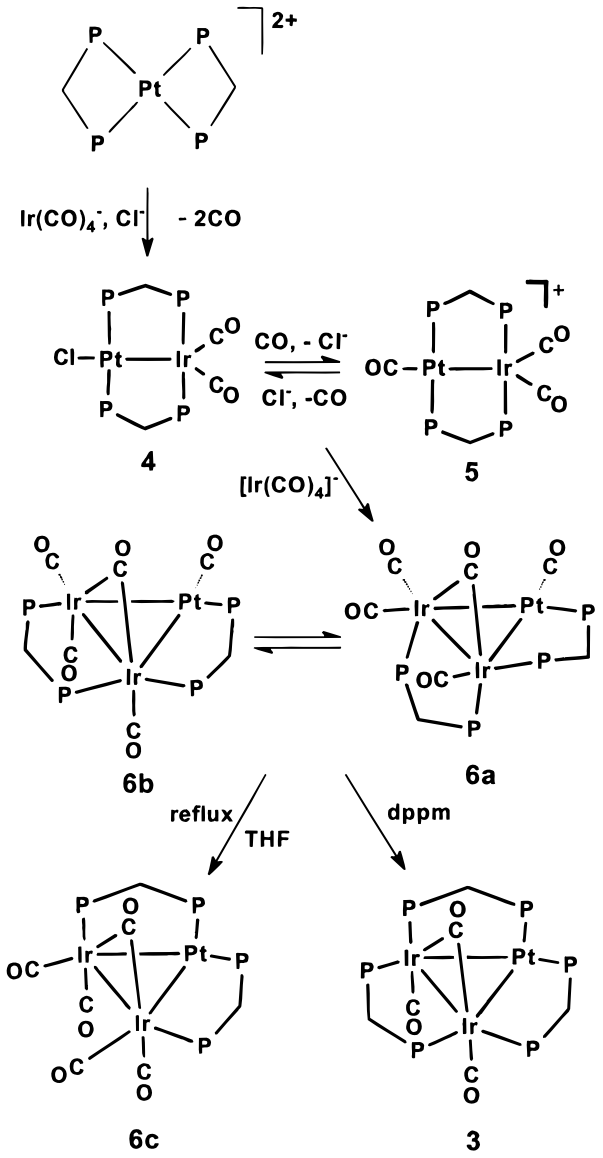

defined in Chart 1. The resonance at δ −16.3 has satellite spectra due to the coupling $^1J(\mathrm{PtP^a}) = 3350$ Hz and is therefore assigned to the Pt-bound phosphine (P^a in Chart 1). This resonance and the resonance at δ −28.6 have a large coupling of 132 Hz in common, assigned as $^3J(\mathrm{P^aP^b})$ between phosphorus atoms trans to the Pt−Ir bonds, and so the resonance at δ −28.6 is assigned to the atoms P^b. The resonance at δ −45.7 is therefore due to P^c. These assignments are in accord with assignments of the ^{31}P NMR spectra of related clusters such as **1** and **2**, and the data are strongly indicative of the presence of a planar $M_3(\mu\text{-dppm})_3$ unit in **3**.[1] The ^{1}H NMR spectrum of the cluster **3** shows four broad resonances in a ratio of 2:2:1:1, assigned to the $\mathrm{CH^aH^bP_2}$ protons of the dppm ligands. Since the structure **3** contains only two different dppm ligands, the observation of four resonances shows that there is no plane of symmetry containing the $Pt_2Ir(PCP)_3$ skeleton so that the $\mathrm{CH^aH^b}$ protons of each dppm ligand are nonequivalent. The resonances with intensity 2 are then assigned to the two equivalent dppm ligands which bridge the Pt−Ir bonds, while the resonances with intensity 1 are due to the dppm ligand which bridges the Ir−Ir bond. The ^{13}C NMR spectrum of a sample enriched with ^{13}CO contained two resonances at δ 196 (terminal IrCO, 2C) and at δ 272 (bridging $Ir_2(\mu\text{-CO})$, 1C), neither of which show resolved coupling to ^{195}Pt. In addition, the IR spectrum of **3** shows three bands at 1944, 1901, and 1610 cm^{-1}, consistent with the presence of two terminal carbonyls and one bridging carbonyl. It should be noted that the bridging carbonyl gives an unusually low value of ν(CO) and an unusually high value of $\delta(^{13}\mathrm{CO})$. It could be argued that these values indicate a triply bridging carbonyl, but the absence of the coupling ^1J(PtC) and the long Pt−C distance (see below) argue against this interpretation. Presumably, the unusual IR and NMR parameters are due to very strong iridium−carbonyl back-bonding in **3**.

Crystals of cluster **3** were of low quality but still gave a well-defined structure. A diagram of the structure is shown in Figure 1, and selected distances and angles are given in Table 1. The three metal atoms form a triangle, each edge of which is bridged by a dppm ligand. The phosphorus atoms of the dppm ligands are roughly coplanar with the $PtIr_2$ triangle. The metal−metal distances are very similar, all falling in the range 2.628(2)−2.673(2) Å. Each iridium atom is bonded to a terminal carbonyl ligand directed perpendicular to the $PtIr_2$ plane, and the third carbonyl symmetrically bridges the two Ir atoms (C(1)−Ir(1) = 2.04(2), C(1)−Ir(2) = 2.05(3) Å); the C(1)−Pt distance of 2.58(2) Å is considered nonbonding.

With this arrangement of the carbonyl ligands, there is an 18-electron configuration at each iridium center and 16-electron configuration at platinum, as expected by analogy to the clusters **1** and **2**. The clusters **1**−**3** have overall electron counts of 42, 44, and 46, respectively. It is interesting that the platinum cluster cation **1** reversibly adds one or two terminal carbonyl ligands to give 44-electron $[Pt_3(CO)_2(\mu\text{-dppm})_3]^{2+}$ and 46-electron $[Pt_3(CO)_3(\mu\text{-dppm})_3]^{2+}$, respectively, which are

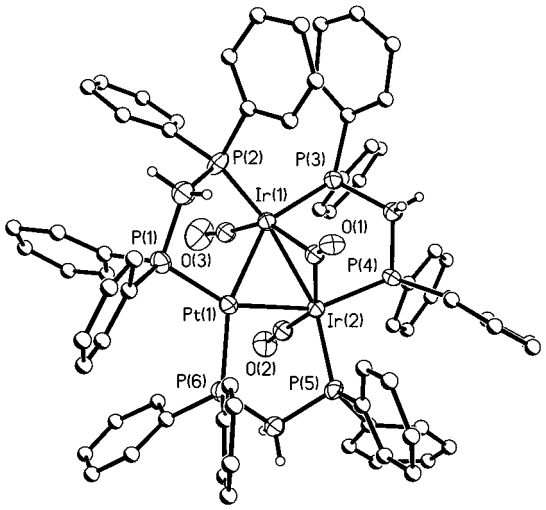

Figure 1. View of the structure of $[PtIr_2(CO)_2(\mu^3\text{-}CO)(\mu\text{-}dppm)_3]$ (**3**). Thermal ellipsoids are drawn at 30% probability, except the phenyl carbons and hydrogens, which are arbitrarily small. The hydrogen atoms of the phenyl groups have been omitted for clarity.

Chart 1

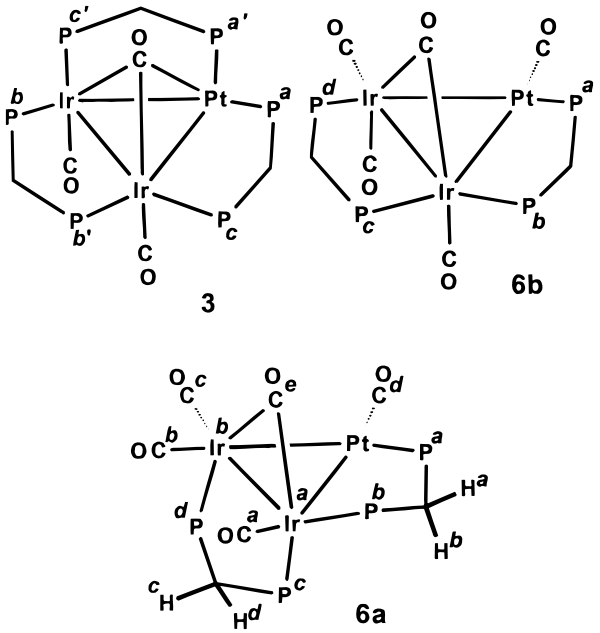

isoelectronic with **2** and **3**, but neither **2** nor **3** reacts with excess CO.[6]

Mechanism of Cluster Formation. Step 1: Formation of Binuclear Pt−Ir Complexes. The reaction to form **3** takes about 24 h, and if the reaction is monitored by ^{31}P NMR spectroscopy, several intermediate compounds can be detected. Each of these compounds has been synthesized and characterized. The initial step in the reaction is the combination of $[Pt(dppm)_2]Cl_2$ with the first equivalent of $PPN[Ir(CO)_4]$ to form a mixture of two heterobimetallic compounds, $[PtIrCl(CO)_2(\mu\text{-}dppm)_2]$ (**4**) and $[PtIr(CO)_3(\mu\text{-}dppm)_2]Cl$ (**5**). Compound **4** was synthesized independently by the reaction of $[Pt(dppm)_2]Cl_2$ with 1 equiv of $PPN[Ir(CO)_4]$.

Table 1. Selected Bond Lengths (Å) and Angles (deg) for $[PtIr_2(CO)_2(\mu\text{-}CO)(\mu\text{-}dppm)_3]$ (3)

Pt(1)−Ir(1)	2.668(2)	Pt(1)−Ir(2)	2.628(2)
Ir(1)−Ir(2)	2.673(2)	Pt(1)−C(1)	2.58(2)
Ir(1)−C(1)	2.04(2)	Ir(1)−C(3)	1.93(3)
Ir(2)−C(1)	2.05(3)	Ir(2)−C(2)	1.91(3)
O(2)−C(2)	1.13(2)	O(1)−C(1)	1.24(2)
O(3)−C(3)	1.13(2)	Pt(1)−P(1)	2.233(8)
Pt(1)−P(6)	2.262(7)	Ir(1)−P(3)	2.281(7)
Ir(1)−P(2)	2.289(8)	Ir(2)−P(5)	2.292(7)
Ir(2)−P(4)	2.306(7)		
Ir(2)−Pt(1)−Ir(1)	60.62(4)	Pt(1)−Ir(2)−Ir(1)	60.43(4)
Pt(1)−Ir(1)−Ir(2)	58.95(4)	P(1)−Pt(1)−Ir(2)	153.4(2)
P(6)−Pt(1)−Ir(2)	96.3(2)	C(1)−Pt(1)−Ir(2)	46.3(6)
P(1)−Pt(1)−Ir(1)	93.5(2)	P(6)−Pt(1)−Ir(1)	156.6(2)
C(1)−Pt(1)−Ir(1)	45.6(5)	C(3)−Ir(1)−Pt(1)	91.4(7)
C(1)−Ir(1)−Pt(1)	65.0(7)	P(3)−Ir(1)−Pt(1)	149.1(2)
P(2)−Ir(1)−Pt(1)	95.4(2)	C(3)−Ir(1)−Ir(2)	97.8(8)
C(1)−Ir(1)−Ir(2)	49.4(7)	P(3)−Ir(1)−Ir(2)	92.1(2)
P(2)−Ir(1)−Ir(2)	148.5(2)	C(2)−Ir(2)−Pt(1)	91.1(8)
C(1)−Ir(2)−Pt(1)	65.7(7)	P(5)−Ir(2)−Pt(1)	92.4(2)
P(4)−Ir(2)−Pt(1)	153.2(2)	C(2)−Ir(2)−Ir(1)	95.9(8)
C(1)−Ir(2)−Ir(1)	48.9(6)	P(5)−Ir(2)−Ir(1)	150.9(2)
P(4)−Ir(2)−Ir(1)	97.8(2)	P(1)−Pt(1)−P(6)	109.8(3)
P(1)−Pt(1)−C(1)	111.8(6)	P(6)−Pt(1)−C(1)	122.0(5)
C(3)−Ir(1)−C(1)	145.8(10)	C(3)−Ir(1)−P(3)	103.8(8)
C(1)−Ir(1)−P(3)	88.6(7)	C(3)−Ir(1)−P(2)	101.1(8)
C(1)−Ir(1)−P(2)	105.4(7)	P(3)−Ir(1)−P(2)	107.5(3)
C(2)−Ir(2)−C(1)	143.8(10)	C(2)−Ir(2)−P(5)	94.6(8)
C(1)−Ir(2)−P(5)	112.9(7)	C(2)−Ir(2)−P(4)	107.7(8)
C(1)−Ir(2)−P(4)	88.4(7)	P(5)−Ir(2)−P(4)	104.6(2)

The ^{31}P NMR spectrum of **4** consists of two multiplets at δ 8.68 and −19.94, assigned in terms of a second-order AA′MM′ spin system that is typical for dppm-bridged bimetallic compounds. The resonance at δ 8.68 has the coupling $^1J(PtP) = 2975$ Hz and so is assigned to the Pt−P-bonded phosphorus atoms, and the Ir−P-bonded phosphorus atoms show the long-range coupling $^2J(PtP) = 245$ Hz. In the ^{1}H NMR spectrum of **4**, the CH_2P_2 protons appeared as an apparent quintet at δ 4.56, indicating the presence of an effective plane of symmetry containing the $PtIr(PCP)_2$ skeleton. The ^{13}C NMR spectrum gave a single carbonyl resonance at δ 181, which appeared as a triplet due to the coupling $^2J(PC)$, with satellite spectra due to the coupling $^2J(PtC) = 51$ Hz, clearly indicating the presence of only terminal IrCO groups. The presence of two CO stretches at ν(CO) 1977 (m) and 1886 (s) cm^{-1} in the IR spectrum indicates that there are two terminal carbonyls and the relative intensities of the IR bands are consistent with a trigonal-bipyramidal geometry at iridium.[7]

Under a CO atmosphere, compound **4** reacts reversibly to form the complex $[PtIr(CO)_3(\mu\text{-}dppm)_2]Cl$ (**5**) by substitution of the chloride ligand on platinum by the carbonyl ligand. Complex **5**, as the $[PF_6]^-$ salt, was synthesized directly by reaction of $[Pt(dppm)_2][PF_6]_2$ with $PPN[Ir(CO)_4]$. The spectroscopy of **5** is very similar to that of **4**, with the exception of an additional band in the IR spectrum at 2030 cm^{-1} due to ν(PtCO) and an additional carbonyl resonance in the ^{13}C NMR spectrum at δ 173, with $^1J(PtC) = 1910$ Hz, due to the platinum−carbonyl group.

Compound **5** has been structurally characterized, and a view of the cation is shown in Figure 2. Selected bond parameters are given in Table 2. The cation contains a *trans,trans*-$PtIr(\mu\text{-}dppm)_2$ group, and the Pt−Ir distance

(6) (a) Ferguson, G.; Lloyd, B. R.; Puddephatt, R. J. *Organometallics* **1986**, *5*, 344. (b) Lloyd, B. R.; Bradford, A.; Puddephatt, R. J. *Organometallics* **1987**, *6*, 424. (c) Puddephatt, R. J.; Manojlović-Muir, Lj.; Muir, K. W. *Polyhedron* **1990**, *9*, 2767.

(7) Lukehart, C. M. *Fundamental Transition Metal Organometallic Chemistry;* Brooks/Cole: Monterey, CA, 1985; pp 78−80.

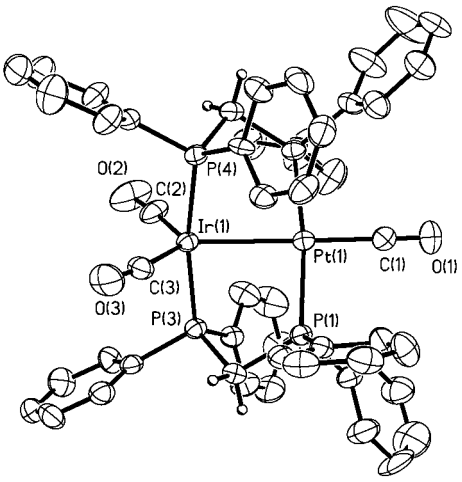

Figure 2. View of the cation $[PtIr(CO)_3(\mu\text{-dppm})_2]^+$ (**5**). Thermal ellipsoids are drawn at 30% probability. The phenyl hydrogen atoms have been omitted.

Table 2. Selected Bond Lengths (Å) and Angles (deg) for $[PtIr(CO)_3(\mu\text{-dppm})_2][PF_6]$ (5)

Pt(1)−C(1)	1.914(9)	Pt(1)−P(1)	2.314(2)
Pt(1)−P(2)	2.317(2)	Pt(1)−Ir(1)	2.7674(4)
Ir(1)−C(3)	1.903(10)	Ir(1)−C(2)	1.905(10)
Ir(1)−P(4)	2.295(2)	Ir(1)−P(3)	2.305(2)
P(1)−C(26)	1.812(8)	P(1)−C(14)	1.817(9)
P(1)−C(4)	1.835(7)	P(2)−C(31)	1.822(9)
P(2)−C(41)	1.835(9)	P(2)−C(5)	1.848(7)
P(3)−C(51)	1.810(9)	P(3)−C(61)	1.828(9)
P(3)−C(4)	1.839(7)	P(4)−C(71)	1.802(8)
P(4)−C(5)	1.810(8)	P(4)−C(81)	1.815(7)
O(1)−C(1)	1.118(9)	O(2)−C(2)	1.129(9)
O(3)−C(3)	1.131(9)		
C(1)−Pt(1)−P(1)	93.6(3)	C(1)−Pt(1)−P(2)	93.9(3)
P(1)−Pt(1)−P(2)	172.33(7)	C(1)−Pt(1)−Ir(1)	179.1(3)
P(1)−Pt(1)−Ir(1)	87.20(5)	P(2)−Pt(1)−Ir(1)	85.24(5)
C(3)−Ir(1)−C(2)	120.0(4)	C(3)−Ir(1)−P(4)	88.9(3)
C(2)−Ir(1)−P(4)	93.3(3)	C(3)−Ir(1)−P(3)	92.9(3)
C(2)−Ir(1)−P(3)	95.3(3)	P(4)−Ir(1)−P(3)	168.92(7)
C(3)−Ir(1)−Pt(1)	123.1(2)	C(2)−Ir(1)−Pt(1)	116.7(3)
P(4)−Ir(1)−Pt(1)	83.89(5)	P(3)−Ir(1)−Pt(1)	86.00(5)
O(1)−C(1)−Pt(1)	176.2(9)	O(2)−C(2)−Ir(1)	173.6(10)
O(3)−C(3)−Ir(1)	172.3(9)		

of 2.7674(4) Å is consistent with the presence of a single bond between these atoms. In addition, the platinum and iridium atoms are bound to one and two terminal carbonyl ligands, respectively, leading to overall square-planar stereochemistry at platinum and trigonal-bipyramidal stereochemistry at iridium. The stereochemistry at iridium is only slightly distorted from ideal trigonal bipyramidal; for example, the angles between the equatorial groups on iridium (2C + Pt) are in the range 116.7(3)−123.1(2)°, all close to the ideal 120°. The P−Pt−P and P−Ir−P axes are twisted by about 40° relative to each other, as is common in binuclear complexes containing $M_2(\mu\text{-dppm})_2$ groups.[8] Clearly, in **5** the platinum atom carries a positive charge and has a 16-electron configuration, while the iridium atom is neutral and has an 18-electron configuration.

Step 2: Formation of the Trinuclear Core. The next step in the formation of the cluster is the addition of the second iridium atom. Reaction of either of the bimetallic complexes **4** and **5** with 1 equiv of [PPN]-$[Ir(CO)_4]$ leads initially to the trimetallic cluster $[PtIr_2(CO)_4(\mu\text{-CO})(\mu\text{-dppm})_2]$ (**6a**). The reaction occurs regioselectively by insertion of iridium into a Pt−P bond. Mechanistically, it is likely that $[Ir(CO)_4]^-$ displaces either the chloride from **4** or the Pt−CO group from **5** to give a complex with a terminal $Pt-Ir(CO)_4$ group, followed by loss of CO from iridium and migration of a phosphine group from platinum to iridium to allow formation of the $PtIr_2$ triangle. In this initially formed complex **6a**, the spectroscopic evidence indicates that one dppm ligand lies in the plane and the other is perpendicular to the plane of the $PtIr_2$ triangle, as shown in Scheme 2.

The ^{31}P NMR spectrum of **6a** contains 4 resonances at δ 2.9 (P^c), −8.0 (P^b), −30.4 (P^a), and −53.7 (P^d), assigned as shown in Chart 1. Only P^a shows a large coupling due to $^1J(PtP) = 3000$ Hz, while the other three resonances show long-range coupling to ^{195}Pt with $^2J(PtP) = 24-92$ Hz, indicating that one phosphorus atom is bound to platinum and the other three are bound to iridium. The coupling $^3J(P^cP^d) = 44$ Hz is much less than that expected if P^d were in the $PtIr_2$ plane, since such values for a trans coupling across a metal−metal bond are typically >100 Hz.[1] The ^1H NMR spectrum is also unusual in having one $CH^cH^dP_2$ proton at the unusual chemical shift of $\delta(H^d) = 7.0$ (the normal range is δ 3−5); the resonance was obscured by phenyl group resonances but was identified in a COSY spectrum by its coupling to H^c at δ 3.31. This resonance is assigned to the proton (of the dppm ligand which bridges the Ir−Ir bond) labeled H^d in Chart 1, which lies directly below the $PtIr_2$ triangle.[5b,9] The other dppm ligand has more usual chemical shifts for the CH^aH^b protons of δ 4.97 and 3.01, and the second of these has satellite spectra due to $^3J(PtH^a) = 130$ Hz, thus showing that this dppm ligand bridges the Pt−Ir bond. The only problem in assigning the stereochemistry of **6a** is the observation of the relatively large coupling $^2J(P^bP^c) = 256$ Hz for the two phosphorus atoms bound to Ir^a; this value is larger than commonly observed for mutually cis phosphorus atoms while smaller than usually observed for mutually trans phosphorus donors[10] and so suggests a distortion of the stereochemistry at Ir^a such that the angle $P^b-Ir^a-P^c$ is ≫90°, probably to reduce steric hindrance between phenyl substituents on P^b and P^c. The ^{13}C NMR spectrum of **6a** shows five resonances for the five inequivalent carbonyl ligands. The three terminal Ir carbonyls appear at δ 170.5 (C^a), 174.1 (C^b), and 181.9 (C^c) (Chart 1); the assignments are tentative, based on the observation of the couplings $^2J(C^aP^b) = 27$ Hz and $^2J(PtC^b) = 52$ Hz (trans coupling through the PtIr bond), while C^c shows no large coupling. The terminal PtCO group gives a resonance at δ 186 with $^1J(PtC^d) = 1460$ Hz, while the bridging carbonyl appears at δ 233.0, with couplings $^2J(P^cC^e) = 48$ Hz and $^2J(P^dC^e) = 38$ Hz, but no coupling to ^{195}Pt.

In solution, **6a** reacts to form an equilibrium mixture with its isomer **6b**, which is assigned a structure with both μ-dppm ligands in the plane of the metal triangle as shown in Scheme 2. The ^{31}P NMR spectrum of **6b** again contains four phosphine resonances at δ −24.8

(8) Manojlović-Muir, Lj.; Muir, K. W.; Solomun, T. *Acta Crystallogr.* **1979**, *B35*, 1237.

(9) Friebolin, H. *Basic One- and Two-Dimensional NMR Spectroscopy;* VCH: Weinheim, Germany, 1993.

(10) Hilts, R. W.; Franchuck, R. A.; Cowie, M. *Organometallics* **1991**, *10*, 1297.

Scheme 3

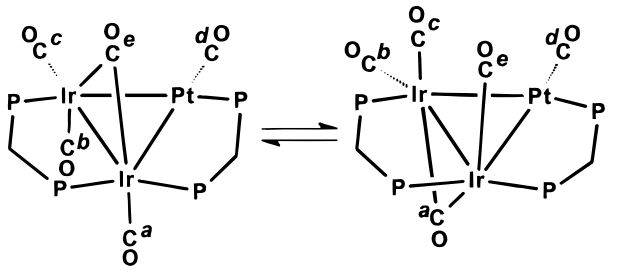

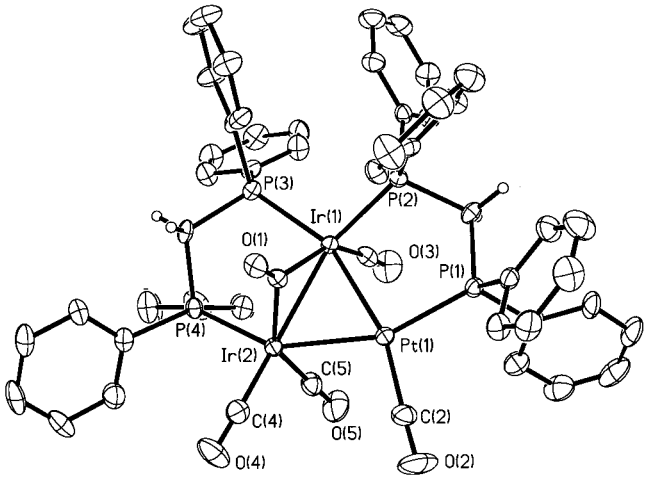

Figure 3. View of the structure of $[PtIr_2(CO)_4(\mu\text{-CO})(\mu\text{-dppm})_2]$ (**6b**). Thermal ellipsoids are shown at 30% probability. Note the similarity to the structure of **3**.

(P^a), −31.1 (P^c), −34.2 (P^d), and −50.0 (P^b), assigned as shown in Chart 1. In contrast to isomer **6a**, the coupling $^3J(P^aP^d) = 128$ Hz for **6b** is in the range expected for a trans coupling across the platinum−iridium bond, while the coupling $^2J(P^cP^d) = 11$ Hz clearly indicates that these phosphorus atoms are mutually cis.

The ^{13}C NMR spectrum of **6b** contains only three carbonyl resonances rather than the expected five (Chart 1), while the ^1H NMR spectrum contains only two resonances due to CH_2P_2 protons rather than the expected four. The apparent symmetry arises as a result of the fluxional process shown in Scheme 3. This process leads to effective equivalence of the pairs of carbonyl ligands C^a,C^e (δ_{av} 226.5) and C^b,C^c (δ_{av} 179.1) while the platinum carbonyl C^d (δ 182.5, $^1J(PtP) = 1610$ Hz) remains fixed in position. This fluxionality was not frozen out even at −90 °C, though some peak broadening was observed; this indicates a particularly low activation energy for carbonyl migration since C^a and C^e are expected to have a difference in chemical shift of >60 ppm. This fluxional process also leads to an effective plane of symmetry containing the $PtIr_2(PCP)_2$ skeleton and so is consistent with the observation of only two resonances for the CH_2 protons of the dppm ligands.

Cluster **6b** has also been characterized by an X-ray structure determination. A view of the molecule is shown in Figure 3, and bond distances and angles are given in Table 3. The three metal atoms form a nearly equilateral triangle with metal−metal distances in the range 2.6305(3)−2.6810(4) Å. The Ir−Ir and Pt−Ir(1) edges are bridged by dppm ligands which are in the plane of the metal triangle, and the carbonyl ligands

Table 3. Bond Lengths (Å) and Angles (deg) for $[PtIr_2(CO)_4(\mu\text{-CO})(\mu\text{-dppm})_2]$ (6b)

Pt(1)−C(2)	1.866(7)	Pt(1)−P(1)	2.275(2)
Pt(1)−Ir(1)	2.6305(3)	Pt(1)−Ir(2)	2.6642(4)
Ir(1)−C(3)	1.915(9)	Ir(1)−C(1)	2.065(8)
Ir(1)−P(2)	2.295(2)	Ir(1)−P(3)	2.315(2)
Ir(1)−Ir(2)	2.6810(4)	Ir(2)−C(4)	1.877(9)
Ir(2)−C(5)	1.915(8)	Ir(2)−C(1)	2.071(6)
Ir(2)−P(4)	2.301(2)	P(1)−C(11)	1.834(7)
P(1)−C(21)	1.838(8)	P(1)−C(6)	1.845(6)
P(2)−C(41)	1.820(7)	P(2)−C(31)	1.831(7)
P(2)−C(6)	1.849(6)	P(3)−C(51)	1.828(7)
P(3)−C(7)	1.835(7)	P(3)−C(61)	1.843(6)
P(4)−C(81)	1.818(8)	P(4)−C(71)	1.832(8)
P(4)−C(7)	1.849(6)	O(1)−C(1)	1.192(8)
O(2)−C(2)	1.140(8)	O(3)−C(3)	1.135(9)
O(4)−C(4)	1.158(10)	O(5)−C(5)	1.144(8)
C(2)−Pt(1)−P(1)	102.3(3)	C(2)−Pt(1)−Ir(1)	163.4(3)
P(1)−Pt(1)−Ir(1)	94.26(4)	C(2)−Pt(1)−Ir(2)	102.6(3)
P(1)−Pt(1)−Ir(2)	154.85(4)	Ir(1)−Pt(1)−Ir(2)	60.837(11)
C(3)−Ir(1)−C(1)	149.2(3)	C(3)−Ir(1)−P(2)	94.2(2)
C(1)−Ir(1)−P(2)	111.0(2)	C(3)−Ir(1)−P(3)	101.9(2)
C(1)−Ir(1)−P(3)	88.6(2)	P(2)−Ir(1)−P(3)	105.27(6)
C(3)−Ir(1)−Pt(1)	91.0(2)	C(1)−Ir(1)−Pt(1)	70.9(2)
P(2)−Ir(1)−Pt(1)	93.24(4)	P(3)−Ir(1)−Pt(1)	156.40(5)
C(3)−Ir(1)−Ir(2)	99.9(2)	C(1)−Ir(1)−Ir(2)	49.7(2)
P(2)−Ir(1)−Ir(2)	149.86(5)	P(3)−Ir(1)−Ir(2)	97.78(5)
Pt(1)−Ir(1)−Ir(2)	60.20(1)	C(4)−Ir(2)−C(5)	103.3(3)
C(4)−Ir(2)−C(1)	103.7(3)	C(5)−Ir(2)−C(1)	145.9(3)
C(4)−Ir(2)−P(4)	100.2(2)	C(5)−Ir(2)−P(4)	103.4(2)
C(1)−Ir(2)−P(4)	91.9(2)	C(4)−Ir(2)−Pt(1)	106.6(2)
C(5)−Ir(2)−Pt(1)	82.6(2)	C(1)−Ir(2)−Pt(1)	70.0(2)
P(4)−Ir(2)−Pt(1)	150.45(5)	C(4)−Ir(2)−Ir(1)	151.4(2)
C(5)−Ir(2)−Ir(1)	99.1(3)	C(1)−Ir(2)−Ir(1)	49.5(2)
P(4)−Ir(2)−Ir(1)	91.49(5)	Pt(1)−Ir(2)−Ir(1)	58.960(10)
O(1)−C(1)−Ir(1)	141.7(5)	O(1)−C(1)−Ir(2)	137.4(6)
Ir(1)−C(1)−Ir(2)	80.8(3)	O(2)−C(2)−Pt(1)	177.6(7)
O(3)−C(3)−Ir(1)	175.5(7)	O(4)−C(4)−Ir(2)	177.9(7)
O(5)−C(5)−Ir(2)	174.9(7)		

PtC(2)O(2) and Ir(2)C(4)O(4) also lie in this plane. In addition, there are two terminal carbonyl ligands Ir(1)C(3)O(3) and Ir(2)C(5)O(5) which lie perpendicular to the $PtIr_2$ plane. An additional carbonyl symmetrically bridges the two iridium atoms on the face opposite to these carbonyls, with distances Ir(1)−C(1) = 2.071(6) Å and Ir(2)−C(1) = 2.065(8) Å. There are obvious similarities between the structures of **6b** and **3**, which differ only in replacement of a bridging dppm ligand in **3** by two terminal carbonyl ligands in **6b**.

If the mixture of isomers **6a** and **6b** is heated under reflux for prolonged periods, a third compound which is believed to be another isomer of **6** is formed. The ^{31}P NMR spectrum of this compound contains only two resonances; therefore, it is thought to be the symmetrical isomer **6c,** in which the dppm ligands both bridge Pt−Ir bonds (Scheme 2). Unfortunately, the complex could not be isolated in pure form because of extensive decomposition which accompanies the slow reaction, and so the proposed structure is tentative.

In solution, **6a** and **6b** exist in a 50:50 mixture, but slow crystallization results in crystals of pure **6b**, presumably due to its lower solubility. If a solid sample of pure **6b** is redissolved, the equilibrium mixture of **6a** and **6b** is again obtained after several hours. The formation of **6a** as the kinetic product in the reaction of **4** with $[Ir(CO)_4]^-$ is likely a result of the previous trans arrangement of the dppm ligands in the binuclear complex. The absence of the symmetrical isomer **6c** in the reaction results because the preferred site for nucleophillic attack by $[Ir(CO)_4]^-$ on the binuclear

complex **4** or **5** is at the coordinatively unsaturated platinum atom, resulting in displacement of Cl^- or CO by $[Ir(CO)_4]^-$ followed by loss of carbonyl ligands and insertion of iridium into a Pt−P bond. This naturally leads to **6a** and not **6c**. Formation of **6c** would require attack by $[Ir(CO)_4]^-$ at the coordinatively saturated iridium center in **4** or **5**, followed by insertion into an Ir−P bond.

Step 3: Addition of the Third dppm Ligand. The final step in the cluster formation is the substitution of the third dppm ligand to bridge the second Pt−Ir bond by displacement of carbonyl ligands from these metal atoms. Both **6a** and **6b** were shown to react easily with dppm to form the cluster **3**. In the case of **6a**, the out-of-plane dppm ligand moves to the in-plane position during the substitution. Again it is likely that a phosphorus atom of the incoming dppm molecule first adds to the coordinatively unsaturated platinum center of **6**, followed by CO loss and coordination of the second phosphorus atom to iridium.

Conclusions

The cluster complex $[PtIr_2(CO)_2(\mu\text{-CO})(\mu\text{-dppm})_3]$ (**3**) is readily synthesized by the reaction of $[Pt(dppm)_2]Cl_2$, $[Ir(CO)_4]^-$, and dppm. The cluster formation proceeds by way of dppm-bridged heterobinuclear Pt−Ir-bonded complexes, which can also be isolated under appropriate experimental conditions. The mechanism defined by Scheme 2 is clearly capable of extension. For example, addition of a new carbonyl anion to **4** or **5** might give clusters containing three different metal atoms, or addition of $[Ir(CO)_4]^-$ to one of many known coordinatively unsaturated binuclear dppm-bridged complexes might lead to new heteronuclear clusters containing iridium.

Cluster **3** is the third in a series of analogous trimetallic clusters, ranging from the dicationic, 42-electron cluster $[Pt_3(\mu_3\text{-CO})(\mu\text{-dppm})_3]^{2+}$ (**1**)[6] to the cationic, 44-electron cluster $[Pt_2Ir(CO)(\mu_3\text{-CO})(\mu\text{-dppm})_3]^+$ (**2**)[1b] to the neutral 46-electron cluster $[PtIr_2(CO)_2(\mu\text{-CO})(\mu\text{-dppm})_2]$ (**3**). The series illustrates two effects. The most obvious is the trend in electron count and structure, arising from the tendency of platinum and iridium to have 16- and 18-electron configurations, respectively. However, a second trend is that the presence of iridium atoms reduces the reactivity of the platinum centers toward further ligand addition. Thus, cluster **1** reversibly adds CO to give 44-electron $[Pt_3(\mu_3\text{-CO})(CO)(\mu\text{-dppm})_3]^{2+}$ and 46-electron $[Pt_3(\mu\text{-CO})(CO)_2(\mu\text{-dppm})_3]^{2+}$, which are isostructural with **2** and **3,** respectively, but neither **2** nor **3** reacts with CO. It is particularly noteworthy that **2** fails to add CO to give a 46-electron cluster; this could just be a charge effect (**2** is a monocation, **1** is a dication), or it could be due to differences in the nature of the metal−metal bonding. In terms of the relationship to bimetallic Pt−Ir catalysts, these results suggest that iridium at the bimetallic surface might become coordinatively saturated and so reduce the effective size of active platinum clusters or that the presence of neighboring iridium might reduce the reactivity of neighboring platinum atoms by Pt−Ir bonding effects.

The clusters **6a** and **6b** are unusual for late-transition-metal clusters in having a triangle of metal atoms with only two μ-dppm ligands, which are still thermally robust. Complexes with the more common $M_3(\mu\text{-dppm})_3$ unit can only react at positions perpendicular to the M_3 triangle, but complexes such as **6** having the $M_3(\mu\text{-dppm})_2$ unit also have two labile carbonyl ligands in the plane and are less sterically hindered. They may therefore exhibit higher reactivity and prove to be particularly versatile models for supported platinum catalysts. The binuclear PtIr clusters described here are of interest because few such complexes having Pt−Ir bonds are known[11] and, in view of the interesting chemistry of both diplatinum and diiridium complexes,[12] the heterobinuclear Pt−Ir-bonded complexes can be expected to have interesting properties.

Experimental Section

Infared spectra were recorded as Nujol mulls by using a Perkin-Elmer 2000 FTIR spectrometer. The ^1H, $^{31}P\{^1H\}$, and $^{13}C\{^1H\}$ NMR spectra were recorded using a Varian Gemini 300 NMR spectrometer. The compound $[PPN][Ir(CO)_4]$[5a] was prepared according to literature methods, and $[Pt(dppm)_2]Cl_2$ was prepared by reaction of $[PtCl_2(SMe_2)_2]$[13] with 2 equiv of dppm in CH_2Cl_2. All manipulations were carried out using standard Schlenk techniques under an atmosphere of prepurified argon.

Synthesis of Compounds. $[PtIr_2(CO)_2(\mu\text{-CO})(\mu\text{-dppm})_3]$ (3). The compounds $PPN[Ir(CO)_4]$ (100 mg, 0.119 mmol), $[Pt(dppm)_2]Cl_2$ (61 mg, 0.059 mmol), and dppm (23 mg, 0.059 mmol) were dissolved in CH_2Cl_2 (15 mL), resulting in the formation of a yellow solution. The solution was stirred for 24 h, at which point the color had changed to deep orange. The solvent was removed in vacuo, and the residue was extracted into THF (3 mL) and filtered through Celite. The solvent was removed from the filtrate, and the residue was recrystallized from CH_2Cl_2/pentane. Yield: 70 mg, 65%. Anal. Calcd for $C_{78}H_{66}Ir_2O_3PtP_6$: C, 51.56; H, 3.66. Found: C, 51.53; H, 3.49. IR: ν(CO) 1944 s, 1901 ms, 1610 mb cm^{-1}. NMR in CD_2Cl_2: $\delta(^1H)$ 3.67 [bm, 1H, dppm CH_2], 4.60 [b, 2H, dppm CH_2], 4.64 [bm, 1H, dppm CH_2], 5.59 [b, 2H, dppm CH_2]; $\delta(^{13}C)$ 196 [2C, terminal CO], 272 [1C, bridging CO]; $\delta(^{31}P)$ −16.3 [dm, $^3J(P^aP^b)$ = 132 Hz, $^1J(P^aPt)$ = 3350 Hz, P^a], −28.6 [dm, $^3J(P^aP^b)$ = 132 Hz, P^b], −45.7 [m, P^c].

$[PtIrCl(CO)_2(\mu\text{-dppm})_2]$ (4). The compounds $[Pt(dppm)_2]Cl_2$ (276 mg, 0.048 mmol) and $PPN[Ir(CO)_4]$ (224 mg, 0.048 mmol) were dissolved in acetone (25 mL) which had been degassed with two freeze−pump−thaw cycles. The white solids dissolved gradually to form a yellow solution, which slowly changed color to golden yellow. After 3 h of stirring, the solvent was removed in vacuo, and the residue was extracted into THF/Et_2O (3 mL/6 mL) and the extract filtered through Celite. The solvent was removed in vacuo, and the residue was recrystallized from CH_2Cl_2/pentane. Yield: 255 mg, 76%. Anal. Calcd for $C_{52}H_{44}ClIrO_2PtP_4$: C, 50.06; H, 3.55; Cl, 2.84. Found: C, 49.86; H, 3.59; Cl, 2.78. IR(Nujol): ν(CO) 1977 (mb), 1886 (sb) cm^{-1}. NMR in acetone-d_6: $\delta(^1H)$ 4.56 [m, ^3J(PtH) = 58 Hz, dppm CH_2]; $\delta(^{13}C)$ 181.0 [t, $^2J(PC)$ = 14 Hz, $^2J(PtC)$ = 51 Hz, Ir*C*O]; $\delta(^{31}P)$ 8.68 [m, $^1J(PtP)$ = 2975 Hz, Pt*P*], −19.94 [m, $^2J(PtP)$ = 245 Hz, Ir*P*].

$[PtIr(CO)_3(\mu\text{-dppm})_2][PF_6]$ (5). The compounds $[Pt(dppm)_2][PF_6]_2$ (74 mg, 0.059 mmol) and $PPN[Ir(CO)_4]$ (50 mg, 0.059

(11) (a) McEwan, D. M.; Markham, D. P.; Pringle, P. G.; Shaw, B. L. *J. Chem. Soc., Dalton Trans.* **1986**, 1809. (b) Markham, D. P.; Shaw, B. L.; Thornton-Pett, M. *J. Chem. Soc., Chem. Commun.* **1987**, 1005. (c) Carr, S. W.; Pringle, P. G.; Shaw, B. L. *J. Organomet. Chem.* **1988**, *341*, 543.

(12) (a) Chaudret, B.; Delavaux, B.; Poilblanc, R. *Coord. Chem. Rev.* **1988**, *86*, 191. (b) Puddephatt, R. J. *Chem. Soc. Rev.* **1983**, *12*, 99.

(13) Hill, G. S.; Irwin, M. J.; Levy, C. J.; Rendina, L. M.; Puddephatt, R. J. *Inorg. Synth.* **1998**, *32*, 149.

Table 4. Crystal Data and Structure Refinement Parameters

	3	5	6a
empirical formula	$C_{78.25}H_{66.5}Cl_{0.5}Ir_2O_3P_6Pt$	$C_{53}H_{44}F_6IrO_{3.5}P_5Pt$	$C_{56}H_{46}Cl_2Ir_2O_5P_4Pt$
fw	1837.85	1393.02	1573.20
temp (K)	294(2)	294(2)	294(2)
wavelength (Å)	0.710 73	0.710 73	0.710 73
space group	$P2_1/n$	*Ccca*	$P\bar{1}$
a (Å)	12.905(1)	20.1924(3)	13.1864(3)
b (Å)	17.315(2)	44.891(1)	13.5273(6)
c (Å)	32.573(3)	23.3886(8)	17.0829(6)
α (deg)	90	90	76.184(2)
β (deg)	101.215(6)	90	77.205(2)
γ (deg)	90	90	67.111(2)
V (Å^3)	7140(1)	21 201(1)	2697.7(2)
Z	4	16	2
ρ(calcd) (Mg/m^3)	1.710	1.746	1.937
abs coeff (mm^{-1})	5.874	5.359	7.772
θ range (deg)	1.27−22.50	1.41−25.00	1.24−25.00
no. of rflns/indep rflns	20 673/9260	9345/9345	15 004/9376
abs cor	semiempirical	semiempirical	semiempirical
no. of data/restrs/params	9217/0/583	9313/0/632	8741/0/632
GOF on F^2	0.935	1.011	0.998
final R1 ($I > 2\sigma(I)$)	0.0692	0.0414	0.0335
wR2 ($I > 2\sigma(I)$)	0.1330	0.0798	0.0616
largest diff peak, hole (e Å^{-3})	1.845, −1.042	1.145, −0.642	2.171, −1.160

mmol) were dissolved in acetone (15 mL) which had been degassed with two freeze−pump−thaw cycles. The white solids dissolved gradually to form a yellow solution, which gradually changed color to orange. The solvent was removed in vacuo, and the residue was extracted into THF (10 mL). Et_2O (10 mL) was then added, resulting in the slow formation over 3 h of an orange microcrystalline solid. The solid was isolated and then extracted into THF (10 mL) and the extract filtered to remove PPN[PF_6]. Addition of 15 mL of Et_2O resulted in the gradual formation of an orange microcrystalline solid, which was isolated and washed with 3 × 10 mL of Et_2O and dried in vacuo. Yield: 50 mg, 61%. Satisfactory analysis could not be obtained because traces of PPN[PF_6] could not be removed from the product, but single crystals could be obtained and the compound was characterized by structure determination. IR(Nujol): *ν*(CO) 2030 (ms), 1977 (s), 1923 (sb) cm^{-1}. NMR in acetone-d_6: *δ*(^{1}H) 5.7 [m, ^1J(PtH) = 57 Hz, dppm CH_2]; *δ*(^{13}C) 173.0 [s, ^1J(PtC) = 1185 Hz, Pt*C*O], 188.8 [s, Ir*C*O]; *δ*(^{31}P) = −7.4 [m, ^1J(PtP) = 1909 Hz, Pt*P*], −20.2 [m, Ir*P*].

[$PtIr_2(CO)_4(\mu$-CO)(μ-dppm)$_2$] (6a,b). The compound [PtIrCl(CO)$_2$(μ-dppm)$_2$] (**4**) was prepared in situ by the reaction of [Pt(dppm)$_2$]Cl$_2$ (50 mg, 0.048 mmol) and PPN[Ir(CO)$_4$] (41 mg, 0.048 mmol) in acetone as described above. The solvent was removed, and additional PPN[Ir(CO)$_4$] (50 mg) was added to the flask. The mixture was dissolved in CH_2Cl_2 (15 mL) and stirred for 12 h to give an orange solution. The solvent was removed in vacuo, and the residue was extracted into THF (3 mL) and filtered. The volume of solvent was reduced to ∼1 mL, and the product was precipitated as a mixture of the two isomers by the addition of Et_2O (10 mL) and pentane (20 mL). Yield: 50 mg, 70%. Anal. Calcd for $C_{55}H_{44}Ir_2O_5P_4Pt$: C, 44.38; H, 2.97. Found: C, 44.17; H, 2.98. If the reaction is carried out in situ in CD_2Cl_2 solvent, the isomer **6a** is observed as the initial product but, after about 24 h in solution, an equilibrium ratio of approximately 1:1 is obtained. Isolation of the product as a solid increases the relative amount of isomer **6b**. When the solid sample is redissolved, it returns over 24 h to the equilibrium ratio. NMR of **6a** in CD_2Cl_2: *δ*(^{1}H) 3.01 [m, 1H, ^2J(H^{a}H^c) = 11 Hz,^3J(PtH) = 130 Hz, *H*^{a}], 3.31 [m, 1H, ^2J(H^{b}H^d) = 13 Hz, *H*^{b}], 4.97 [m, 1H, ^2J(H^{a}H^c) = 11 Hz, ^3J(PtH) = 130 Hz, H^c], 7.0 [*H*^{d}]; *δ*(^{13}C) 170 [dd, ^2J(P^{b}C) = 27 Hz, ^2J(C^{a}P^b) = 8 Hz, C^a], 174 [d, ^3J(P^{c}C) = 36 Hz, ^2J(PtC) = 52 Hz, C^b], 182 [dm, ^2J(C^{c}C^e) = 6, ^2J(C^{c}P^d) = 6, C^c], 186 [s, ^1J(PtC) = 1460 Hz, C^d], 233 [ddd, ^2J(P^{a}C) = 48 Hz, 2J(P^{d}C) = 38 Hz, ^2J(C^{c}C^e) = 6 Hz, C^e]; *δ*(^{31}P) 2.9 [ddd, ^2J(PtP) = 43 Hz, ^2J(P^{a}P^b) = 256 Hz, ^2J(P^{a}P^d) = 17 Hz, ^3J(P^{a}P^c) = 4 Hz, P^a], −8.0 [ddd, ^2J(PtP) = 92 Hz, ^2J(P^{a}P^b) = 256 Hz, ^2J(P^{b}P^c) = 13 Hz, ^3J(P^{b}P^d) = 6 Hz, P^b], −30.4 [ddd, ^1J(PtP) = 3000 Hz, ^2J(P^{c}P^d) = 44 Hz, ^2J(P^{b}P^c) = 13 Hz, ^3J(P^{a}P^c) = 4 Hz, P^c]; −53.7 [ddd, ^2J(PtP) = 24 Hz, ^2J(P^{c}P^d) = 44 Hz, ^2J(P^{a}P^d) = 17 Hz, ^3J(P^{b}P^d) = 6 Hz, P^d]. NMR of **6b** in CD_2Cl_2: *δ*(^{1}H) 5.41 [m, 2H, CH_2], 4.60 [m, 2H, CH_2]; *δ*(^{13}C) 179.1 [s, IrCO], 182.5 [d, ^3J(CP^b) = 37 Hz, ^1J(PtC) = 1610 Hz, PtCO], 226.5 [s, IrCO]; *δ*(^{31}P) −24.8 [dd, ^3J(P^{a}P^c) = 128 Hz, ^2J(P^{a}P^d) = 39 Hz, ^1J(PtP) = 3070 Hz, P^a], −31.1 [dd, ^3J(P^{b}P^c) = 33 Hz, ^2J(P^{b}P^d) = 11 Hz, ^2J(PtP) = 16 Hz, P^b], −34.2 [dd,^3J(P^{a}P^c) = 128, ^3J(P^{b}P^c) = 33, ^2J(PtP) = 50 Hz, P^c], −50.0 [dd, ^2J(P^{a}P^d) = 39 Hz, ^2J(P^{b}P^d) = 11 Hz, P^d]. IR of mixture of **6a** and **6b**: *ν*(CO) 2008 s, 2000 s, 1984 s, 1970 sh, 1943 s, 1935 sh, 1900 sh, 1892 s (terminal CO) cm^{-1}; 1721 s, 1665 s (bridging CO) cm^{-1}.

X-ray Data Collection and Structure Solution. Crystal data and refinement parameters for **3**, **5**, and **6a** are listed in Table 4. Data were collected using a Nonius Kappa-CCD system. Unit cell parameters were calculated from reflections obtained from 10−15 consecutive data images collected at *φ* intervals of 1° using COLLECT (Nonius, 1998) or DENZO v. 1.9 (Nonius, 1997). One full hemisphere of data was collected by incremental *φ* scans of 1° followed by 1° *ω* scans to capture cusp data. Data were scaled using SCALEPACK (Nonius, 1997), and empirical absorption corrections were applied using XPREP in SHELXTL 5.03. Full-matrix least-squares refinement on F^2 was performed after solution using Patterson methods and the solution package SHELXTL 5.03.

Crystals of **3** were grown by diffusion of pentane into a saturated CH_2Cl_2 solution. A crystal, of marginal quality, was mounted on a glass fiber. Systematic absences and intensity data indicated the monoclinic space group $P2_1/c$, and this choice was borne out by successful refinement of the structure. Anisotropic thermal parameters were applied to the metal atoms, all phosphorus atoms, and the oxygen atoms only. The phenyl rings were constrained to idealized regular hexagons, and isotropic thermal parameters were used; 0.25 molecule of CH_2Cl_2 was located in the lattice. The largest residual peak was found in the lattice and was associated with the heavy metal core (1.845 e Å^{-3}).

Crystals of **5** were grown by diffusion of diethyl ether into a saturated solution of methylene chloride. A crystal suitable for X-ray analysis was cut to the appropriate size and mounted on a glass fiber. Systematic absences indicated the uniquely determined orthorhombic space group *Ccca*, and this was borne out by successful refinement of the structure. Anisotropic thermal parameters were applied to all non-hydrogen atoms

except the fluorine atoms of PF_6^- and the disordered water molecule in the lattice. Atoms C(45) and C(46) were disordered over two positions and refined with site occupancy factors of 0.5. The largest residual peak was located between Pt(1) and Ir(1) (1.145 e $Å^{-3}$).

Crystals of **6b** were grown from a saturated solution of methylene chloride, and a crystal suitable for X-ray analysis was mounted on a glass fiber. A statistical analysis of intensity data indicated the triclinic space group $P\bar{1}$, and this was borne out by successful refinement of the structure. Empirical absorption corrections were applied using redundant data and XPREP (SHELXTL 5.03). Anisotropic thermal parameters were applied to all non-hydrogen atoms. The largest residual peak was found between the three heavy metal atoms (2.171 e $Å^{-3}$).

Acknowledgment. We thank the NSERC of Canada for financial support.

Supporting Information Available: Tables of X-ray data, in CIF format, are available. Access information is given on any current masthead page.

OM980665Y